Quantitative Analysis of Planar Technetium-99m-Sestamibi Myocardial Perfusion Images Using Modified Background Subtraction

Kenneth Koster, Frans J. Th. Wackers, Jennifer A. Mattera, and Robert C. Fetterman

Yale University School of Medicine, Cardiovascular Nuclear Imaging Laboratory, Department of Diagnostic Radiology, Department of Internal Medicine (Section of Cardiology), New Haven, Connecticut

Standard interpolative background subtraction, as used for thallium-201 (^{201}Tl), may create artifacts when applied to planar technetium-99m-Sestamibi (^{99m}Tc-Sestamibi) images, apparently because of the oversubtraction of relatively high extra-cardiac activity. A modified background subtraction algorithm was developed and compared to standard background subtraction in 16 patients who had both exercise-delayed ^{201}Tl and exercise-rest ^{99m}Tc-Sestamibi imaging. Furthermore, a new normal data base was generated. Normal ^{99m}Tc-Sestamibi distribution was slightly different compared to ^{201}Tl. Using standard background subtraction, mean defect reversibility was significantly underestimated by ^{99m}Tc-Sestamibi compared to ^{201}Tl (2.8 ± 4.9 versus −1.8 ± 8.4, $p < 0.05$). Using the modified background subtraction, mean defect reversibility on ^{201}Tl and ^{99m}Tc-Sestamibi images was comparable (2.8 ± 4.9 versus 1.7 ± 5.2, p = NS). We conclude, that for quantification of ^{99m}Tc-Sestamibi images a new normal data base, as well as a modification of the interpolative background subtraction method should be employed to obtain quantitative results comparable to those with ^{201}Tl.

J Nucl Med 1990; 31:1400–1408

Technetium-99m hexakis-2-methoxy-isobutyl isonitrile (^{99m}Tc-Sestamibi) is a new radiopharmaceutical which recently has been introduced (*1*) and evaluated for exercise-rest myocardial perfusion imaging. Preliminary clinical trials have demonstrated that ^{99m}Tc-Sestamibi exercise-rest planar imaging is comparable to thallium-201 (^{201}Tl) imaging for detection of coronary artery disease (*2–8*). In these comparative studies, *qualitative or visual* image analysis was employed. Numerous reports have shown that *quantitative* image analysis significantly enhances reproducibility, reliability, and diagnostic yield of planar ^{201}Tl stress imaging (*9–17*). Therefore, clinical validation of a new myocardial perfusion agent should also include *quantitative image analysis.*

Our initial attempts to apply the ^{201}Tl quantitative analysis method (*7*) to ^{99m}Tc-Sestamibi images showed occasional artifactual and erroneous defects (*18,19*). Figure 1 shows an example of a reversible ^{201}Tl defect, both by visual and quantitative analysis. The ^{99m}Tc-Sestamibi images of the same patient show a similar *reversible* defect by visual inspection. However, after computer quantification, the graphic display of circumferential count distribution profiles incorrectly shows a *fixed* defect. Figure 2 shows a visually *normal* ^{99m}Tc-Sestamibi image, which is abnormal by computer quantification.

We hypothesized that oversubtraction of background in the interpolative subtraction algorithm was responsible for these findings (*18–21*). The source of oversubtraction was thought to be due to the relatively high subdiaphragmatic uptake of ^{99m}Tc-Sestamibi adjacent to the heart compared to ^{201}Tl images (*5*). Accordingly, a modification of the background subtraction algorithm was designed by Watson and Smith, which adjusted for relatively high non-cardiac radioactivity (*19,22*). In addition, a new normal ^{99m}Tc-Sestamibi data base was established.

In this report, we compared this modified quantitative algorithm to the standard algorithm previously used for ^{201}Tl in exercise-rest ^{99m}Tc-Sestamibi studies. Because of lack of an independent clinical criterion for myocardial perfusion abnormalities, in particular for myocardial ischemia, the quantitative results with ^{99m}Tc-Sestamibi were compared to those with ^{201}Tl in the same patients. The results demonstrate that the proposed modification successfully corrects for background oversubtraction and provides comparable quantification of ^{99m}Tc-Sestamibi and ^{201}Tl images.

Received Sept. 11, 1989; revision accepted Feb. 8, 1990.

For reprints contact: Frans J. Th. Wackers, MD, Director, Cardiovascular Nuclear Imaging and Exercise Laboratories, Yale University School of Medicine, 333 Cedar Street, TE-2, New Haven, CT 06510.

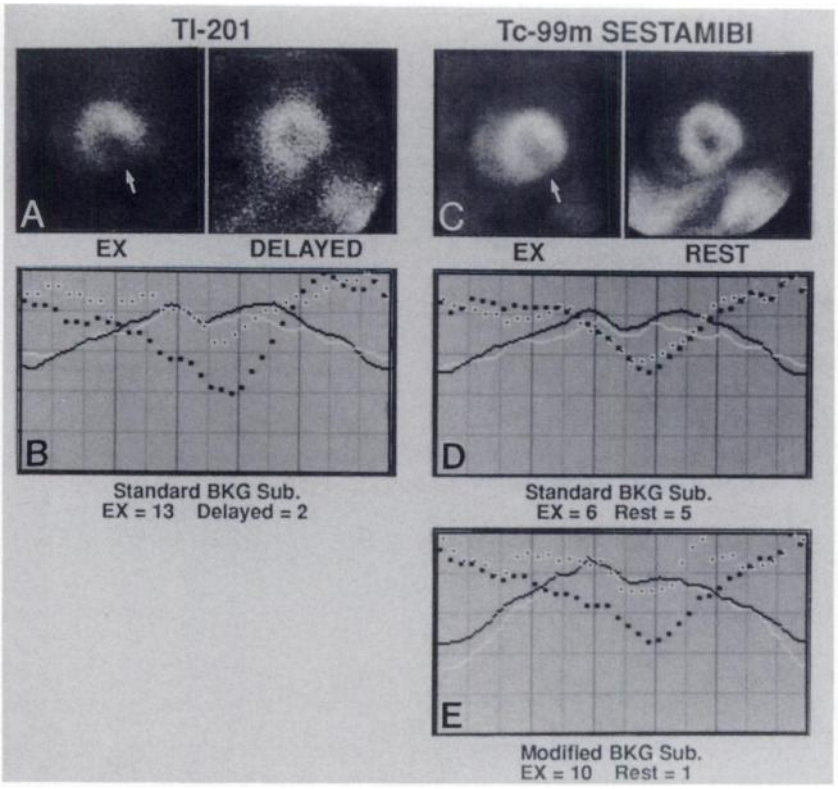

FIGURE 1
Thallium-201 and ^{99m}Tc Sestamibi images (LAO view) of the same patient. (A) A reversible inferolateral ^{201}Tl defect (arrow) is present. (B) Employing standard background subtraction, the circumferential profiles show a reversible defect (exercise defect 13, delayed defect 2). (C) The ^{99m}Tc Sestamibi images are comparable to those obtained with ^{201}Tl: a reversible inferolateral defect (arrow). Note the high subdiaphragmatic activity at rest. (D) Employing standard background subtraction, the circumferential profiles erroneously display a fixed defect (exercise defect 6, rest defect 5). (E) Employing modified background subtraction (see text), the circumferential profiles display correctly a reversible defect comparable to B (exercise defect 10, rest defect 1). Black dots = post-exercise data; white dots with black center = delayed or rest data; solid black line = lower limit of normal distribution (in [D] for ^{201}Tl, in [E] for ^{99m}Tc-Sestamibi); and EX = exercise.

METHODS AND STUDY SELECTION

Selection of Patient Studies

For comparative analysis, 16 pairs of planar ^{201}Tl and ^{99m}Tc-Sestamibi images were selected from a larger data base acquired in the course of a Phase III multicenter trial to establish diagnostic efficacy of ^{99m}Tc-Sestamibi stress imaging. In this trial, patients with angiographic coronary artery disease (CAD) had both planar exercise-delayed ^{201}Tl imaging and exercise-rest ^{99m}Tc-Sestamibi imaging. The study pairs were selected using criteria required for adequate quantitative processing of myocardial perfusion images:

1. Adequate count density (at least 30K counts in the background corrected left ventricular region).
2. Adequate dimensions around the heart in the field of view for appropriate positioning of the reference region for background subtraction.
3. *Similar perfusion abnormalities* on the ^{201}Tl and ^{99m}Tc-Sestamibi images by *visual inspection.*

Since it was our purpose to validate a modification of the processing algorithm, studies with marked visually discordant information were excluded. Thirty-nine of 60 available paired

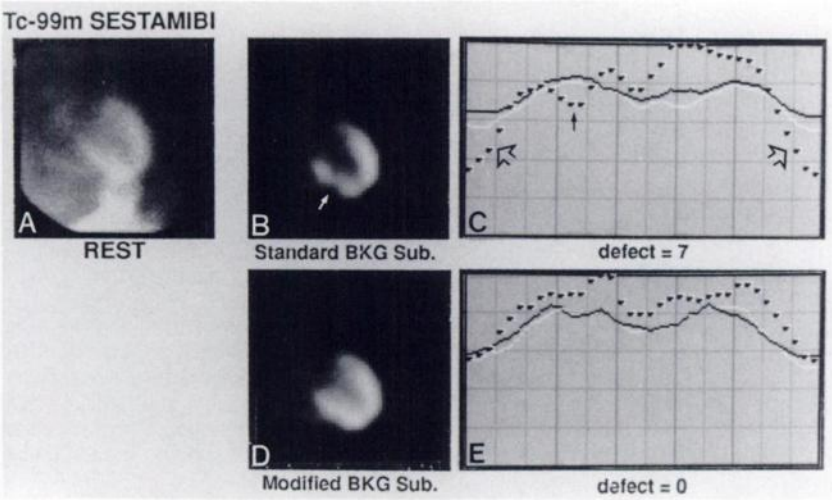

FIGURE 2
(A) Normal resting ^{99m}Tc-Sestamibi image (ANT view). Note high subdiaphragmatic activity. (B) The same image after standard background correction. Note (erroneous) defect (arrow) due to oversubtraction. (C) Circumferential profiles after standard background subtraction and curve for lower limit of ^{201}Tl distribution (solid black line). The circumferential profiles are below normal at the valve planes (open arrows) and in the inferoseptal segments (arrow). (D) The same image as in A after modified background subtraction. The image appears visually normal. (E) Circumferential profiles after modified background subtraction and display of the lower limit of normal ^{99m}Tc-Sestamibi distribution (solid black line). The circumferential profiles are at all points above the lower limit curve, indicating correctly a normal distribution of ^{99m}Tc-Sestamibi.

studies were rejected for insufficient count density, zoomed acquisition, or suboptimal technical quality on either ^{201}Tl or ^{99m}Tc-Sestamibi images. Of the 21 resulting study pairs, 5 studies were excluded because of marked discrepancies in the visual analysis between ^{201}Tl and ^{99m}Tc-Sestamibi images. The remaining 16 pairs of studies constitute the study group.

Individuals for the Normal Data Base

A normal ^{99m}Tc-Sestamibi data base was generated from 18 healthy subjects with a low likelihood (<5%) of CAD who underwent treadmill exercise with ^{201}Tl and subsequently with ^{99m}Tc-Sestamibi. The likelihood of CAD was determined using stepwise probability analysis as described by Diamond and Forrester on the basis of age, sex, absence of symptoms, normal physical exam, and normal exercise/rest ECG (*23*). A normal data base for ^{201}Tl studies (n = 27) has been previously established employing similar criteria (*7*). The lower limits of normal distribution of both imaging agents were defined as the mean minus 2 standard deviations (s.d.).

Myocardial Imaging Protocol

Informed consent was obtained from all patients. Thallium-201 exercise imaging was performed at least one day prior to ^{99m}Tc-Sestamibi exercise imaging. The ^{201}Tl exercise test was symptom limited and approximately the same heart rate/systolic blood pressure double product was reproduced for the ^{99m}Tc-Sestamibi exercise test. Treadmill exercise was performed following the standard Bruce protocol. At peak exercise, a bolus of 92.5 MBq (2.5 mCi) of ^{201}Tl was injected intravenously. The patient was encouraged to continue exercising at the same level for at least 1–2 min. Planar ^{201}Tl stress imaging was started within 5 min of injection at peak exercise and the delayed images were obtained 2–3 hr later (no late redistribution or resting ^{201}Tl imaging was performed).

Planar ^{99m}Tc-Sestamibi imaging was performed following two *separate* (interval at least 24 hr) intravenous injections of 740 MBq (20 mCi) of ^{99m}Tc-Sestamibi. Technetium-99m-Sestamibi images were acquired 1 hr after injection, either during exercise or at rest.

Planar myocardial images were obtained in the left anterior oblique (LAO), left lateral (LLAT), and anterior (ANT) projections, without cranial or caudal tilt. Rigid quality control was employed to ensure the best reproducibility of imaging projections. Planar imaging was performed using standard gamma cameras equipped with a low-energy-all-purpose collimator. The energy windows were centered asymmetrically over the 68–80 keV ^{201}Tl X-rays (25% @ 80 keV), and symmetrically over the 167 keV (20%) photopeak of ^{201}Tl. A 20% window was symmetrically centered on the 140 keV photopeak of ^{99m}Tc. All images were acquired on a minicomputer using a 128 × 128 matrix in word mode.

Modification of Background Subtraction Algorithm for Sestamibi Images

Interpolative background subtraction, as used for quantitative ^{201}Tl imaging, involves the generation of a nonuniform background image (*24,25*). In brief, a boundary or reference region is placed around the heart. For each pixel within this region, background is computed from the symmetrical weighted average of count density at four orthogonal boundary points (*25*). Thus, a background image is created for the exercise and delayed image. The background image is then subtracted from the raw images. This process is repeated for exercise and delayed images. The standard background algorithm proposed by Goris and modified by Watson (*24,25*) computes the background with a *gradual* "fall-off" from high to low extra-cardiac background. This algorithm will be referred to as *standard background subtraction.*

It was hypothesized that the relatively high accumulation of ^{99m}Tc-Sestamibi in subdiaphragmatic organs was the cause of oversubtraction in adjacent myocardial regions. Consequently, the algorithm was modified (see Appendix) once more by Watson and Smith to create an initial *steeper* fall-off and then leveling-out with a more homogeneous background subtraction over the cardiac region (*26*) (see Fig. 3). The latter

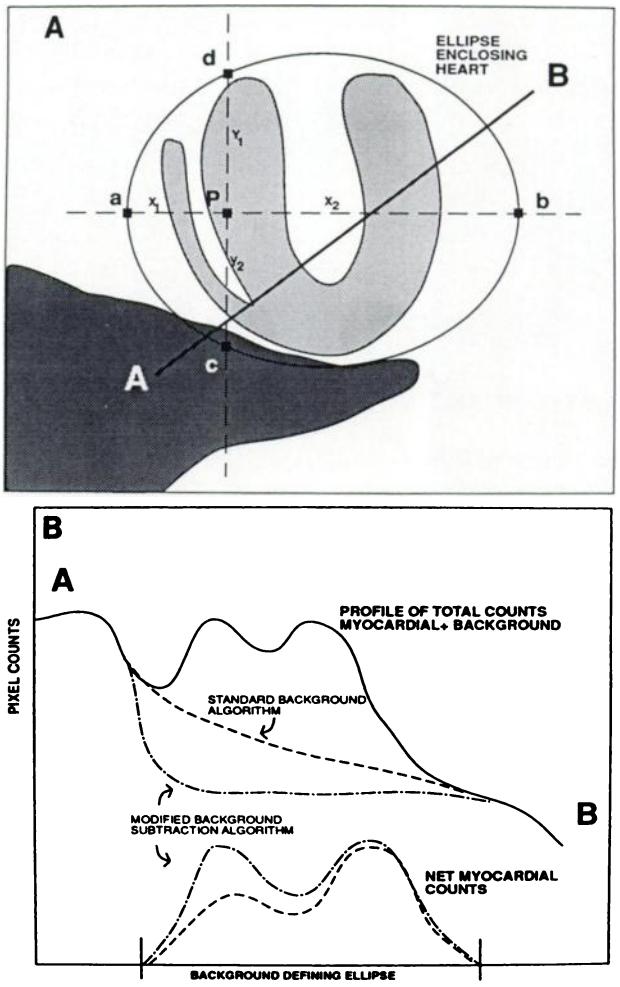

FIGURE 3
(A) Schematic representation of characteristic distribution of ^{99m}Tc-Sestamibi at rest. In addition to uptake in the heart, accumulation of the radiopharmaceutical in the liver is shown. To generate an interpolated background image, the operator places an ellipse around the heart. For each pixel within this region, the background value is calculated (see Appendix). (B) Schematic representation of count profile (top) along line A to B on the schematic ^{99m}Tc-Sestamibi image in Figure A. The more rapid "fall-off" with the modified background subtraction in comparison to the standard background subtraction algorithm is shown. Bottom: Net myocardial count profiles after standard and modified subtraction are shown. The oversubtraction adjacent to the heart is corrected.

modification will be referred to as *modified background subtraction.*

Quantification of Images

The method for quantification of ^{201}Tl perfusion images has been described previously (*9*). In brief, circumferential count distribution profiles were generated from mean pixel counts in 36 segments (10° each) of the left ventricle. The circumferential distribution profiles were graphically displayed against a curve representing the lower limits of normal (mean minus 2 s.d.) derived from normal data bases (27 subjects for ^{201}Tl, 18 subjects for ^{99m}Tc-Sestamibi). In a normal myocardial perfusion image, all data points of the circumferential profile are at or above this lower limit. A myocardial perfusion defect is graphically displayed as a portion of the circumferential profile *below* the lower limit of normal (Fig. 4).

A myocardial perfusion defect is quantitated as the integral of the area below the lower limit of normal in proportion to the total potentially visualized normal myocardium. The potentially visualized normal myocardium assumes the normal value of ^{201}Tl counts in the area of the defect to be at least equal to the lower limit of normal distribution. The defect integral is unitless (fractional unit) and reflects both the extent (number of angles) and severity (depth) of the defect below the lower limit boundary. The reproducibility of quantification of defect size has been reported previously (*21*).

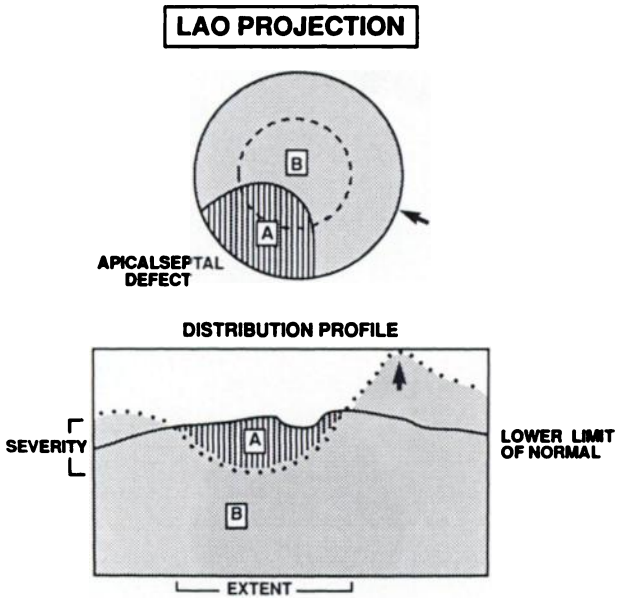

FIGURE 4
Quantification of perfusion defect. The schematic diagram shows an apical septal defect (A) on a LAO image. The left ventricle (A + B) is divided into 36 10° segments. A circumferential distribution profile (black dots) is generated by plotting the mean count density of each segment. The segment with the highest mean count density is assigned 100% (arrow) and the other segments are plotted as a percentage of this maximal value. This profile is superimposed on a curve (solid black line) indicating the lower limit of normal (mean − 2 s.d.) distribution of the radiopharmaceutical. The defect integral is calculated by expressing the defect (A) as proportion (×100) of the total potentially visualized normal myocardium:

$$\frac{A}{A + B} \times 100 \text{ (see text).}$$

Processing

All ^{201}Tl and ^{99m}Tc-Sestamibi studies were processed independently, using the appropriate normal data base for the standard background subtraction and the modified background subtraction. An identical region of interest over the left ventricle was used to generate the circumferential profiles for comparison of the two background subtraction methods.

Comparison of Circumferential Profiles

The four sets of quantitated studies (^{201}Tl and ^{99m}Tc-Sestamibi studies processed each with standard and modified background subtraction) were separated. Each set was interpreted by two experienced observers without knowledge of the interpretation of the other sets. Each three-view study was categorized from the circumferential profiles by visual judgment as "normal" (both exercise and delayed/rest profiles above the lower limit of normal), "reversible defect" (a segment of the exercise profile is below the lower limit with a visually estimated considerable [>25%] improvement of the delayed/rest profile), or a "fixed defect" (no difference between the exercise and delayed/rest profiles).

Quantitative Comparison of Defect Size

Since the assessment of reversibility of defects from circumferential profiles is subjective and involves intraobserver variability, the data are also presented strictly numerically. The *total defect size* on a three-view study is defined as the algebraic sum of the defect integrals on 3 views after exercise and at delayed imaging or at rest. The *difference* between the total exercise defect and the total delayed or resting defect is a measure of the degree of reversibility of the defect.

Statistical Analysis

The data are expressed as mean ± s.d. Paired data were compared by two-tailed, paired t-test. The relative size of the exercise defects on ^{201}Tl and ^{99m}Tc-Sestamibi images and the relative rank order in the defect size were compared by Spearman Rank Correlation Coefficient. A probability (p) of <0.05 was considered to be statistically significant.

RESULTS

Technetium-99m-Sestamibi Normal Distribution: Comparison to Thallium-201

Figure 5 shows the comparison of lower limits of normal (mean − 2 s.d.) for ^{201}Tl and ^{99m}Tc-Sestamibi images using the modified background algorithm. Point-by-point calculation of the t-value of the difference between the mean of normal myocardial distribution of ^{201}Tl and ^{99m}Tc-Sestamibi indicated only statistically significant deviations in the valve plane regions on the ANT and LAO views. Correlation coefficients between ^{201}Tl and ^{99m}Tc-Sestamibi were 0.94, 0.92, and 0.98 for ANT, LAO, and LLAT views, respectively.

Patient Studies

Interpretation of Circumferential Profiles. Figures 1 and 2 show the effect of modification of the interpolative background algorithm and of employing a new

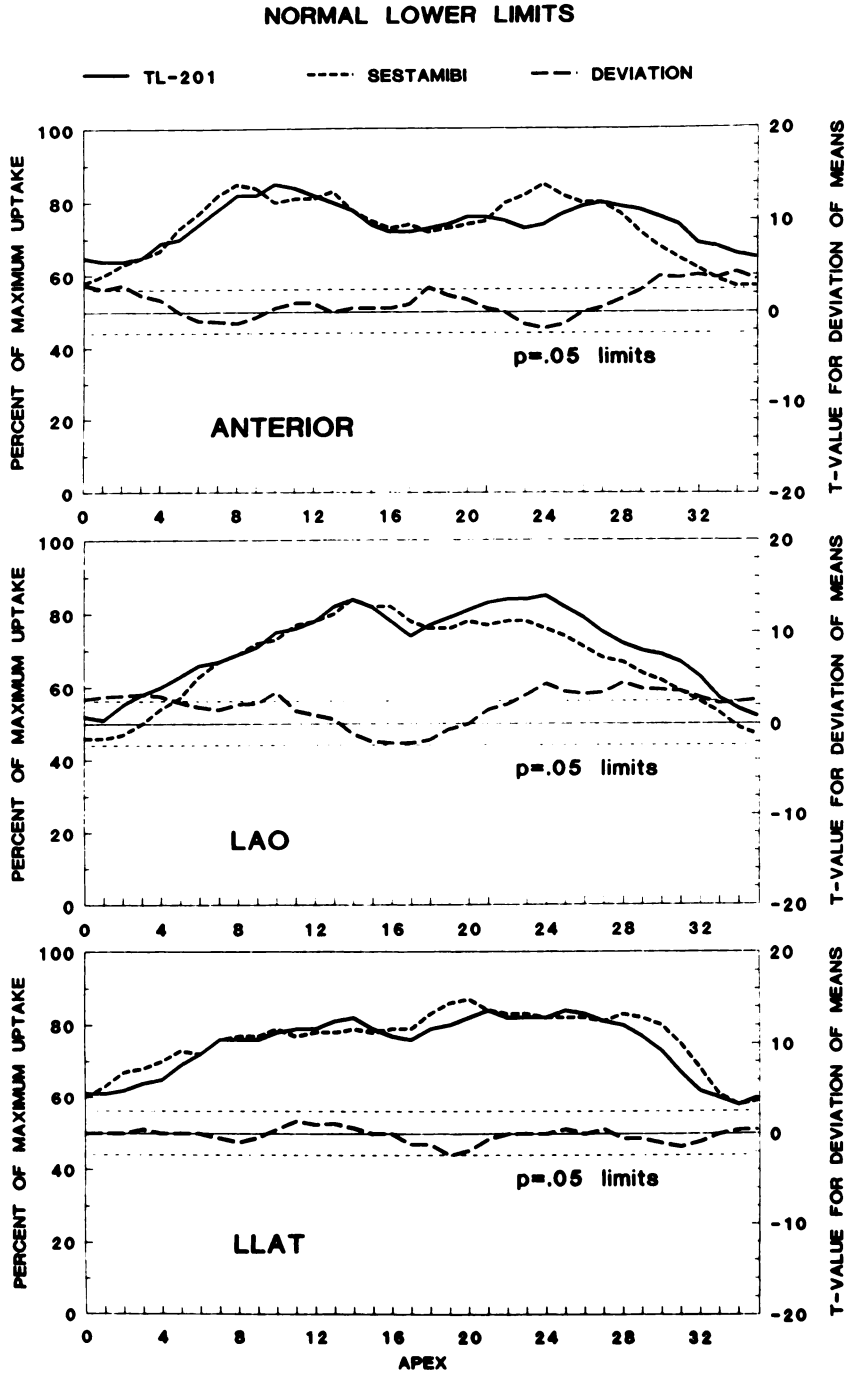

FIGURE 5
Lower limits of normal count distribution (mean – 2 s.d.) for ^{201}Tl and ^{99m}Tc-Sestamibi images in the anterior (ANT), left anterior oblique (LAO) and left lateral (LLAT) projections using the modified background subtraction. Statistical deviations for the mean values are shown with the p = 0.05 limits for t-values. Statistically significant deviations between ^{201}Tl and ^{99m}Tc-Sestamibi values occur in the valve plane regions on the ANT and LAO views.

normal ^{99m}Tc-Sestamibi data base in two patient studies.

The results of interpretation of circumferential profiles of 16 paired ^{201}Tl and ^{99m}Tc-Sestamibi studies using both background subtraction methods are shown in Figure 6. There was no difference in interpretation of the ^{201}Tl studies using either background subtraction method. Employing the standard background subtraction method, nine patients showed reversible ^{201}Tl defects of whom only four patients showed reversible defects by ^{99m}Tc-Sestamibi. Two patients with fixed ^{201}Tl defects had reversible ^{99m}Tc-Sestamibi defects. Five patients had normal ^{201}Tl images, and four of these also had normal ^{99m}Tc-Sestamibi images. Overall, concordance was 50%. Using the modified background subtraction, eight of the nine patients with reversible ^{201}Tl defects also had reversible ^{99m}Tc-Sestamibi defects. This improved overall concordance to 75%.

Quantitative Comparison

Standard Background Subtraction (Fig. 7). The mean total defect integral on the ^{201}Tl images after exercise was 7.9 ± 10.7, 6.0 ± 8.5 at delayed imaging, and the mean difference (i.e., reversibility of defect) between

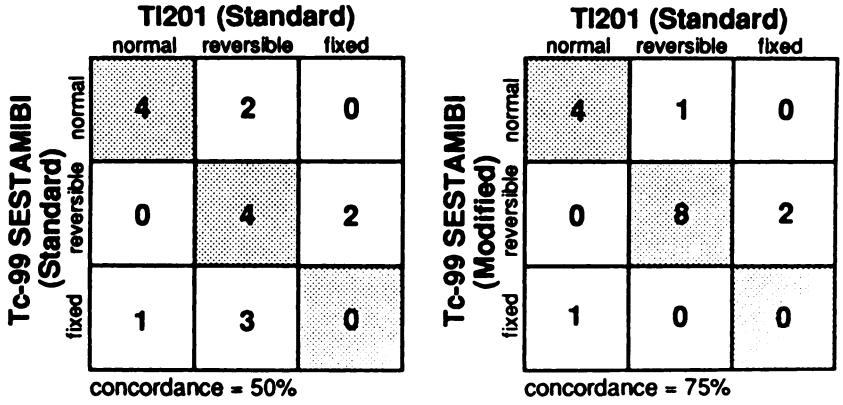

FIGURE 6
Contingency tables of interpretation of circumferential profiles from 16 paired ^{201}Tl and ^{99m}Tc-Sestamibi studies (see text). The ^{201}Tl studies were analyzed with the standard background subtraction and compared to ^{99m}Tc-Sestamibi studies analyzed with either standard or modified background subtraction. The concordance was 50% employing standard background subtraction (and ^{201}Tl lower limits) and improved to 75% employing the modified background subtraction (and ^{99m}Tc-Sestamibi lower limits).

the two was 2.8 ± 4.9, when analyzed using the standard background subtraction.

The mean total defect integral on the ^{99m}Tc-Sestamibi images after exercise was 10.4 ± 12.9 (p = ns compared to ^{201}Tl), 12.2 ± 13.2 at rest imaging (p < 0.05 compared to ^{201}Tl), and the mean difference between the two was −1.8 ± 8.4 (p < 0.05 compared to ^{201}Tl), using the standard background subtraction.

Modified Background Subtraction (Fig. 7). Using the modified background subtraction, the mean total defect integral on the ^{201}Tl images after exercise was 5.6 ± 7.8 (p = ns, compared to ^{201}Tl analyzed with standard background subtraction) and at delayed imaging was 3.4 ± 4.7 (p < 0.05 compared to ^{201}Tl analyzed with standard background subtraction). The mean difference between the two was 2.3 ± 4.0 (p = ns, compared to ^{201}Tl analyzed with standard background subtraction), using the modified background subtraction.

The mean total defect integral on the ^{99m}Tc-Sestamibi images after exercise was 8.6 ± 10.0, 6.8 ± 8.3 at rest imaging, and the mean difference between the two was 1.7 ± 5.2 (p = ns for all three compared to ^{201}Tl using both background subtraction methods), using the modified background subtraction.

Comparative Analysis per View (Fig. 8). On a view-by-view basis, the exercise ^{201}Tl and ^{99m}Tc-Sestamibi defect integrals were not significantly different (p = ns) using either background subtraction method.

Defect Integral Rank Order. Using the modified background subtraction algorithm, the Spearman Rank Order analysis indicated a positive correlation for the size of exercise defects between ^{201}Tl and ^{99m}Tc-Sestamibi on three views(Table 1).

DISCUSSION

The study demonstrates that a well-validated computer algorithm developed for one specific imaging agent, i.e. ^{201}Tl, cannot be employed without further validation for another perfusion imaging agent, such as ^{99m}Tc-Sestamibi. The relatively high subdiaphragmatic uptake of ^{99m}Tc-Sestamibi adjacent to the heart created incorrect quantitative data by oversubtraction in the interpolative background algorithm.

Technetium-99m-Sestamibi images differ from ^{201}Tl images by the marked subdiaphragmatic uptake of radiopharmaceutical in liver, gallbladder, and gastrointestinal system and less low-photon energy scatter. The

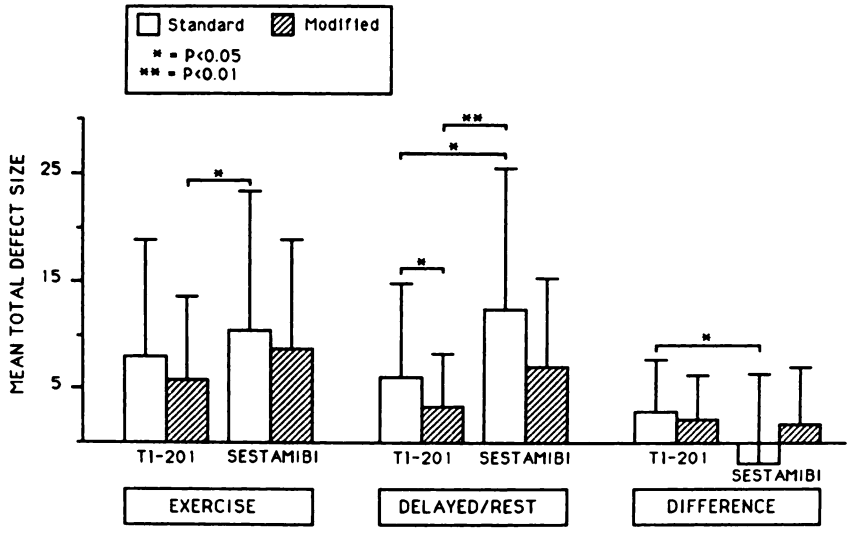

FIGURE 7
Mean (+s.d.) total defect integral in 16 patients after exercise, at rest, and the difference between the two (exercise-rest) using the standard and modified background subtraction method for ^{201}Tl and ^{99m}Tc-Sestamibi. Comparisons were not statistically significant unless indicated (see text).

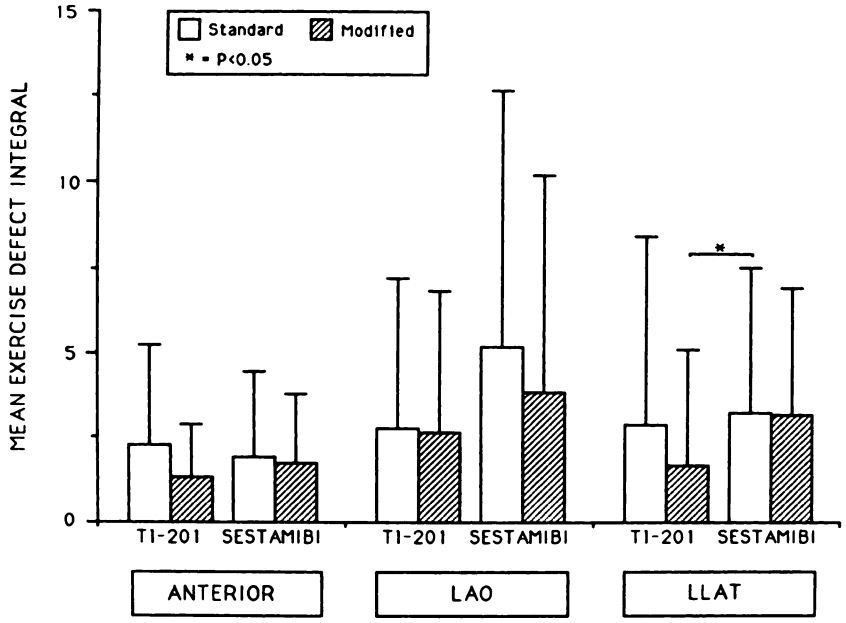

FIGURE 8
Comparison of mean (+s.d.) exercise defect integral on ^{201}Tl and ^{99m}Tc-Sestamibi images in the anterior (ANT), left anterior oblique (LAO), and left lateral (LLAT) projections using the standard and modified background subtraction algorithm. Comparisons were not statistically significant unless indicated (see text).

less marked subdiaphragmatic radioactivity and the greater amount of low-energy scatter on ^{201}Tl images results in a relatively homogeneous background activity and for this reason the more gradual fall-off of the standard interpolative background subtraction algorithm was satisfactory in the clinical practice of ^{201}Tl imaging for a number of years. We had noticed, however, that the computer quantification of some ^{201}Tl studies with increased pulmonary uptake or increased subdiaphragmatic activity (after dipyridamole infusion or on resting studies) at times resulted in unexpected and apparently erroneous data.

The proposed modification of background subtraction involves a steeper fall-off at the site of the relatively high extra-cardiac activity and reaches an earlier plateau of background subtraction (*26*). This new reference background plane was created by inductive reasoning and empirical testing. The present study represents an initial validation of this modification. Unfortunately, no true gold standard for "background" or "exercise-induced myocardial perfusion abnormalities" exists. Therefore, it appeared reasonable to employ a well-established technique such as quantitative ^{201}Tl imaging as a touchstone for comparison.

Comparison of the mean values for normal distribution of ^{201}Tl and ^{99m}Tc-Sestamibi using the modified background subtraction showed small but significant differences at the valve planes in the anterior and left anterior oblique views. This is consistent with the observation that less scatter gives better resolution of the valve plane "defects" with ^{99m}Tc-Sestamibi. Additionally, there was also an indication of more defined "apical thinning" with ^{99m}Tc-Sestamibi. The latter difference did not reach statistical significance.

TABLE 1
Spearman Rank Correlation Coefficients (r_s) for ^{201}Tl and ^{99m}Tc-Sestamibi Exercise Defect Integrals on Three Views Using the Modified Background Subtraction

	^{201}Tl vs. ^{99m}Tc-Sestamibi r_s
Anterior	0.68
Left lateral oblique	0.71
Left lateral	0.66

Circumferential profile analysis showed poor agreement between ^{99m}Tc-Sestamibi and ^{201}Tl images using the standard background subtraction with regard to defect reversibility. The concordance with ^{201}Tl imaging improved considerably using the modified background subtraction algorithm. It is of interest that two patients with fixed ^{201}Tl defects, had reversible defects with ^{99m}Tc-Sestamibi. These two patients had normal regional wall motion on contrast ventriculography. The limitations of ^{201}Tl stress imaging in fully identifying viable myocardium has recently been recognized (*28, 29*). No late redistribution imaging was performed in these patients.

Quantitative comparison on the basis of the defect size demonstrated that the size of exercise ^{201}Tl defects and the difference between exercise and delayed defects, were not significantly influenced by the modification of background subtraction. However, because of greater subdiaphragmatic activity, the resting ^{201}Tl defect size was significantly smaller, using the modified background subtraction. As expected, there was also no statistically significant difference between ^{201}Tl and ^{99m}Tc-Sestamibi exercise defect size using either background subtraction method. Exercise images with both radiopharmaceuticals have relatively low extra-cardiac activity.

However, resting ^{99m}Tc-Sestamibi defects were significantly larger than the corresponding resting ^{201}Tl defects using the standard background subtraction. Furthermore, the amount of reversibility of defects by ^{99m}Tc-Sestamibi imaging was significantly smaller compared to ^{201}Tl. This indicates that myocardial ischemia is systematically underestimated on ^{99m}Tc-Sestamibi studies using the standard background subtraction.

The modification of background subtraction corrected for these differences (Figs. 1 and 2). There was no longer a statistically significant difference between delayed ^{201}Tl and resting ^{99m}Tc-Sestamibi defects nor was there a difference between the amount of the reversibility (Fig. 7).

Thus, the effect of modifying the background subtraction algorithm was particularly striking on the resting ^{99m}Tc-Sestamibi studies. These images frequently have substantial subdiaphragmatic activity. In all instances, the presence of high subdiaphragmatic activity created either an erroneous defect or made an existing defect larger (Fig. 1), using the standard background subtraction. In some normal studies, erroneous defects were created in this manner (Fig. 2). These artifacts appeared to occur on any view, but in particular on the left lateral projection. Noise from intense upper gastrointestinal tract accumulation of radioisotope in this projection may interfere with the signal of the activity of the inferior myocardial wall.

Some have advocated the postponement of imaging to ~60 min after injection of ^{99m}Tc-Sestamibi. At this time, most of the hepatic activity has cleared by biliary excretion. Nevertheless, accumulation of the radiopharmaceutical in the gastrointestinal tract may at times cause considerable problems. It may still be difficult to separate cardiac from lower gastrointestinal activity. Therefore, the time interval between injection and start of imaging can conceivably be individualized with the relative organ distribution as a guide.

Thus far, comparative studies evaluating the detection of CAD by ^{201}Tl and ^{99m}Tc-Sestamibi have been performed by visual analysis alone (*5*). Our present study indicates that by using computer quantification, the diagnostic information (i.e., the presence of defects, defect size, and defect reversibility) is preserved.

Computer quantification improves the reproducibility of interpretation. Quantification of defect size is also important since the magnitude (severity and extent) of exercise defects has been shown to be of clinical and prognostic value (*30–32*). We demonstrated a positive correlation in defect size rank order between ^{201}Tl and ^{99m}Tc-Sestamibi exercise studies. Therefore, it appears that the potential prognostic information obtained from ^{201}Tl imaging also can be obtained from quantitative ^{99m}Tc-Sestamibi imaging. More specifically, patients with the largest ^{201}Tl defects also had the largest ^{99m}Tc-Sestamibi defects.

We recently employed quantitative analysis with the presented modification of background subtraction in patients who had thrombolytic therapy for acute myocardial infarction and serial ^{99m}Tc-Sestamibi imaging (*33*). Quantitative changes in defect size correlated with the status of the infarct related artery. Furthermore, the size of ^{99m}Tc-Sestamibi defects correlated inversely with left ventricular ejection fraction. The same study showed a good correlation between the size of resting ^{99m}Tc-Sestamibi defects and the size of delayed ^{201}Tl defects at predischarge exercise (*33*). Such preliminary data suggest that quantification of ^{99m}Tc-Sestamibi defect size provides meaningful clinical information.

The present study demonstrates that quantification of ^{99m}Tc-Sestamibi images, using the proposed modification of background subtraction and a new normal data base, is comparable to that of ^{201}Tl images. Future clinical evaluation of this new imaging agent should preferably involve quantitative image analysis.

APPENDIX

Generation of Interpolated Background Image (see Fig. 3A–B)

The background value (BkgV) for pixel P for the *modified* background subtraction within the region of interest is calculated with the following formula:

$$\text{BkgV} = \frac{w_a a + w_b b + w_c c + w_d d + 64v}{w_a + w_b + w_c + w_d + 64},$$

where the weighting factors w_a, w_b, w_c and w_d are as follows:

$$w_a = (x_2/x_1)^2 \qquad w_b = (x_1/x_2)^2$$

$$w_c = (y_2/y_1)^2 \qquad w_d = (y_1/y_2)^2.$$

The constant V, is computed as follows: Sort, from smallest to largest, all pixels lying on the boundary of the reference ellipse enclosing the heart, generated for the background subtraction. Find the average of the pixels between the 20th percentile and the 50th percentile. [Formula made available by Dr. Watson and Mr. Smith (*26*).]

ACKNOWLEDGMENTS

The authors express their appreciation for the technical assistance of Diana Errico, RTNM, Edwin Levine, RTNM, Michael McMahon, CNMT, Mark Saari, CNMT, and Gretchen White, CNMT.

Technetium-99m-Sestamibi was kindly supplied by E.I. Du Pont de Nemours, Inc., North Billerica, MA.

The modification of the interpolative background correction algorithm was designed and made available to us by Denny D. Watson, PhD and William H. Smith, MS, University of Virginia, Health Sciences Center, Division of Medical Imaging, Charlottesville, VA.

REFERENCES

1. Jones AG, Abrams MF, Davison A, et al. Biological studies of a new class of technetium complexes: the hexakis (alkylisonitrile) technetium (I) cations. *Int J Nucl Med Biol* 1984; 11:225–234.
2. Holman BL, Jones AG, Lister-James J, et al. A new Tc-99m-labeled myocardial imaging agent, hexakis (t-Butylisonitrile)-technetium(I) [Tc-99mTBI]: initial experience in the human. *J Nucl Med* 1984; 25:1350–1355.
3. Holman BL, Sporn V, Jones AG, et al. Myocardial imaging with technetium-99m CPI: initial experience in the human. *J Nucl Med* 1987; 28:13–18.
4. Deutch E, Vanderheyden JL, Gerundini P, et al. Development of nonreducible technetium-99m(III) cations as myocardial perfusion imaging agents: initial experience in humans. *J Nucl Med* 1987; 28:1870–1880.
5. Wackers FJTh, Berman DS, Maddahi J, et al. Technetium-99m hexakis 2-methoxyisobutyl isonitrile: human biodistribution, dosimetry, safety, and preliminary comparison to thallium-201 for myocardial perfusion imaging. *J Nucl Med* 1989; 30:301–311.
6. Taillefer R, Dupras G, Sporn V, et al. Myocardial perfusion imaging with a new radiotracer, technetium-99m-hexamibi (methoxy isobutyl isonitrile): comparison with thallium-201 imaging. *Clin Nucl Med* 1989; 14:89–98.
7. Kiat H, Maddahi J, Lynne TR, et al. Comparison of technetium-99m methoxyisobutyl isonitrile and thallium-201 for evaluation of coronary artery disease by planar and tomographic methods. *Am Heart J* 1989; 117:1–11.
8. Baillet GY, Mena IG, Kuperus JH, et al. Simultaneous technetium-99m-MIBI angiography and myocardial perfusion imaging. *J Nucl Med* 1989; 30:38–44.
9. Wackers FJTh, Fetterman RC, Mattera JA, et al. Quantitative planar thallium-201 stress scintigraphy: a critical evaluation of the method. *Semin Nucl Med* 1985; 15:46–66.
10. Maddahi J, Garcia EV, Berman DS, et al. Improved noninvasive assessment of coronary artery disease by quantitative analysis of regional stress myocardial distribution and washout of thallium-201. *Circulation* 1981; 64:924–935.
11. van Train KF, Berman DS, Garcia EV, et al. Quantitative analysis of stress thallium-201 myocardial scintigrams: a multicenter trial. *J Nucl Med* 1986; 27:17–25.
12. Berger BC, Watson DD, Taylor GJ, et al. Quantitative thallium-201 exercise scintigraphy for detection of coronary artery disease. *J Nucl Med* 1981; 22:585–593.
13. Massie BM, Hollenberg M, Wisneski JA, et al. Scintigraphic quantification of myocardial ischemia: a new approach. *Circulation* 1983; 68:747–755.
14. Garcia E, Maddahi J, Berman D, et al. Space/time quantification of thallium-201 myocardial scintigraphy. *J Nucl Med* 1981; 22:309–317.
15. Kaul S, Boucher CA, Newell JB, et al. Determination of the quantitative thallium imaging variables that optimize detection of coronary artery disease. *J Am Coll Cardiol* 1986; 7:527–37.
16. Lie SP, Reiber JHC, Simoons ML, et al. Computer processing of thallium-201 myocardial scintigrams. *Proceedings of the second international conference on visual psychophysics and medical imaging.* Silver Spring, MD: IEEE; 1981:(Cat. 81):19–25.
17. Reiber JHC, Lie SP, Simoons ML, et al. Computer quantification of the location, extent and type of thallium-201 myocardial perfusion abnormalities. *Proceedings of the international symposium on medical imaging and image interpretation ISMIII.* Silver Spring, MD: IEEE; 1982:(Cat. 82):123–128.
18. Koster K, Wackers FJ, Fetterman RC. Interpolative background subtraction as used for Tl-201 imaging creates major inaccuracy in quantitative Tc-99m isonitrile imaging [Abstract]. *J Am Coll Cardiol* 1988; 11:33A.
19. Sinusas AJ, Smith WH, Brookman V, et al. Quantitative imaging with Tc-99m methoxyisobutyl isonitrile (RP-30): comparison with Tl-201 using a new background subtraction algorithm [Abstract]. *Circulation* 1987; 76(suppl IV):217.
20. Watson DD, Smith WH, Sinusas AJ, et al. Myocardial defect detection with Tc-99m methoxyisobutyl isonitrile vs Tl-201 [Abstract]. *J Nucl Med* 1988; 29:850.
21. Watson DD, Sinusas AJ, Smith WH, et al. Quantitative methods for myocardial imaging with Tc-99m MIBI [Abstract]. *J Nucl Med* 1988; 29:955.
22. Watson DD, Taillefer R, Smith WH, et al. Quantitative standards for hexamibi [Abstract]. *J Nucl Med* 1988; 30:790.
23. Diamond GA, Forrester JS. Analysis of probability as an aid in the clinical diagnosis of coronary artery disease. *N Engl J Med* 1979; 300:1350–1358.
24. Goris ML, Daspit SG, McLaughlin P, et al. Interpolative background subtraction. *J Nucl Med* 1976; 17:744–747.
25. Watson DD, Campbell NP, Read EK. Spatial and temporal quantitation of plane thallium myocardial images. *J Nucl Med* 1981; 22:577–584.
26. Sinusas AJ, Beller GA, Smith WH, et al. Quantitative planar imaging with technetium-99m methoxyisobutyl isonitrile: comparison of uptake patterns with thallium-201. *J Nucl Med* 1989; 30:1456–1463.
27. Sigal SL, Mattera JA, Fetterman RC, et al. Virtue and limitations of quantification of extent and severity of planar Tl-201 perfusion defects [Abstract]. *J Nucl Med* 1989; 30:863.
28. Kiat H, Berman DS, Maddahi J, et al. Late reversibility of tomographic myocardial thallium-201 defects: an accurate marker of myocardial viability. *J Am Coll Cardiol* 1988; 12:1456–1463.
29. Cloninger KG, DePuey EG, Garcia EV, et al. Incomplete redistribution in delayed thallium-201 single photon emission computed tomography (SPECT) images: an overestimation of myocardial scarring. *J Am Coll Cardiol* 1988; 12:955–963.
30. Brown KA, Boucher CA, Okada RD, et al. Prognostic value of exercise thallium-201 imaging in patients presenting for evaluation of chest pain. *J Am Coll Cardiol* 1983; 1:944–1001.
31. Reisman S, Maddahi J, Van Train K, et al. Quantitation of extent, depth, and severity of planar thallium defects in patients undergoing exercise thallium-201 scintigraphy. *J Nucl Med* 1986; 27:1273–1281.
32. Ladenheim ML, Pollock BH, Rozanski A, et al. Extent and severity of myocardial hypoperfusion as predictor of prognosis in patients with suspected coronary artery disease. *J Am Coll Cardiol* 1986; 7:464–471.
33. Wackers FJ, Gibbons RJ, Verani MS, et al. Serial quantitative planar technetium-99m isonitrile imaging in acute myocardial infarction: efficacy for non-invasive assessment of thrombolitic therapy. *J Am Coll Cardiol* 1989; 14:861–873.